Insight into the Mechanism of a Peptide Inhibitor of HIV Reverse Transcriptase Dimerization†

Julien Depollier,‡ Marie-Laure Hourdou,‡ Gudrun Aldrian-Herrada,‡ Paul Rothwell,§ Tobias Restle,⊥ and Gilles Divita‡

Department of Molecular Biophysics & Therapeutics, Centre de Recherches de Biochimie Macromoléculaire, FRE-2593 CNRS, 1919 Route de Mende, 34293 Montpellier, France, School of Crystallography, Birbeck College, University of London, Malet Street, London WC1E 7HX, U.K., and Institut für Molekulare Medizin, UK S-H Campus of Lubeck, Ratzeburger Allee 160, 23538 Lübeck, Germany

Received July 23, 2004; Revised Manuscript Received September 29, 2004

ABSTRACT: The biologically active forms of human immunodeficiency viruses type 1 and 2 reverse transcriptase (RT) found in infectious virions are heterodimers. We have previously shown that the dimeric nature of reverse transcriptase represents an important target for the design of a new class of antiviral agents and have designed a short peptide (Pep-7) derived from the tryptophan-rich motif of the connection subdomain that blocks dimerization of reverse transcriptase in vitro and abolishes viral infection. In the present work, we have investigated the mechanism through which this peptide inhibits RT dimerization and consequently viral propagation. We demonstrate that Pep-7 interacts preferentially with the p51 subunit within the heterodimeric reverse transcriptase, which destabilizes reverse transcriptase dimer conformation, thereby triggering dissociation. We have identified two residues Trp^{24} and Phe^{61}, located on the fingers subdomain of p51, required for Pep-7 binding. Selective mutation of these residues on p51 to a glycine dramatically alters the stability of the RT-heterodimer suggesting that the fingers subdomain of p51 is also involved in stabilization of reverse transcriptase. We propose that the binding site of Pep-7 is located in a cleft between the fingers and the connection subdomains of p51 that contains the two highly conserved residues Phe^{61} and Trp^{24}.

Among the treatments directed against the etiologic agent responsible for the development of AIDS, human immunodeficiency virus (HIV),[1] there is still a need for new compounds capable of blocking viral propagation efficiently (1,2). There is no doubt that the highly active antiretroviral therapy (HAART) has improved prognosis of HIV infected patients, even though numerous side effects and limitations regarding tolerability remain a concern. The main target of most treatments is reverse transcriptase (RT), an essential enzyme that transcribes viral RNA into DNA, which is then integrated into the infected host genome. Several RT inhibitors have already been developed and are used to treat HIV infections (*1*−*3*). However, the major problem with these inhibitors is associated with the emergence of resistance mutations (*1*−*4*). Therefore identification of new compounds targeting other features of RT remains an important task. The biologically active form of reverse transcriptase is a heterodimer of two subunits, p51 and p66, each consisting of distinct functional subdomains, the fingers, the palm, the thumb, and the connection, as well as an RNase H subdomain, which is only present in p66 (*5*−*8*). We and others have investigated the dimerization of p51 and p66 and have shown that this process, mediated by the interaction between the two connection subdomains, is absolutely essential for RT to acquire the full spectrum of its biological activities (*6, 9*−*13*). We have demonstrated that dimerization of RT is a two-step process involving first the rapid association of the two subunits, followed by a slow conformational change generating the active form of the enzyme (*12*). We and other groups have suggested that dimerization of RT represents an interesting target for the design of more specific inhibitors (*14*−*16*). Several studies have clearly established a direct correlation between the NNRTI binding site and the stability of RT (*17*−*19*), although, the mechanistic pathways involved still remain to be clarified. Some NNRTI are able to alter the stability of the enzyme (*17, 18*) while others improve the formation of dimeric RT (*19*). We have proposed that a short peptide of 10 residues (Pep-7) derived from the tryptophan-rich motif of the connection subdomain of RT (KETWETWWTE; residues 395−404 of HIV-1 BH_{10} RT) constitutes a powerful inhibitor of HIV-1 RT dimerization in vitro and prevents the production of viral particles in HIV-

† This work was supported in part by the Centre National de la Recherche Scientifique (CNRS) and by grants from the Agence Nationale de Recherche sur le SIDA (ANRS), SIDACTION and the Fondation pour la Recherche Médicale (FRM). J.D. was supported by a fellowship form the ANRS. This work was supported by the EC (Grant LSHB-CT-2003-503480) program "Targeting Replication and Integration of HIV "(TRIoH)".

* To whom correspondence should be addressed. Tel: (33) 04 67 61 33 92. Fax: (33) 04 67 52 15 59. E-mail: gilles.divita@crbm.cnrs.fr.

§ University of London.

⊥ UK S-H Campus of Lubeck.

‡ Centre de Recherches de Biochimie Macromoléculaire.

[1] Abbreviations: HIV, human immunodeficiency virus; FAM, 5′-fluorescein phosphoramidite; HAART: highly active antiretroviral therapy; NNRTI, nonnucleoside reverse transcriptase inhibitor; RT, reverse transcriptase; TSAO-T, [2′,5′-bis-*O*-(*tert*-butyldimethylsilyl)-*β*-D-ribofuranosyl]-3′-spiro-5″-(4″-amino-1″,2″-oxathiole-2″,2″-dioxide)thymine; P/T, primer/template.

10.1021/bi0484264 CCC: $30.25
Published on Web 01/20/2005

1_{BRU}-infected cultured CEM cells at very low concentrations (*20*).

In the present work, we have investigated the mechanism through which Pep-7 inhibits RT dimerization. We have shown that binding of Pep-7 mainly affects the conformation of the p51 subunit and have identified two key residues involved in this mechanism, Trp^{24} and Phe^{61} located in the fingers subdomain of p51. This allows us to understand the potency of Pep-7 as a novel anti-HIV therapeutic agent and explains why this compound prevents viral propagation of a variety of isolates of HIV-1.

EXPERIMENTAL PROCEDURES

Materials. Poly(rA)-oligo(dT) and ^{3}H-dTTP (1 μCi/μL) were purchased from Amersham Biosciences, Orsay, France. dTTP was purchased from Roche Molecular Biochemicals, Roche Diagnostics, Meylan, France. Oligonucleotides for mutagenesis and 5′-labeled primer and template oligonucleotides used for fluorescence titration were purchased from MWG Biotech AG, Ebersberg, Germany. MF-membrane (25 mm, 0.45 μm) filters for RT assay were purchased from Millipore, Molshein, France.

Peptides (Pep-7, KETWETWWTE; Pep-77, KETAETAAATE). All peptides were synthesized using an (fluorenylmethoxy)-carbonyl (Fmoc) continuous flow apparatus (Pioneer, Applied Biosystems, Foster City, CA) starting from Fmoc−polyamide linker (PAL)−poly(ethylene glycol) (PEG)−polystyrene (PS) resins at a 0.05 mmol scale. Peptides were purified by semipreparative reversed-phase high-performance liquid chromatography (RP-HPLC; C18 column Interchrom UP5 WOD/25M Uptispere 300 5 ODB, 250 mm × 21.2 mm) and identified by electrospray mass spectrometry. Pep-7 peptide (200 nmol) was coupled to Lucifer yellow iodoacetamide dipotassium (500 nmol) through overnight incubation at 4 °C in 50 mM Tris-buffer, pH 7.3. Fluorescently labelled peptide was further purified by RP-HPLC using a C18 reverse-phase HPLC column (Interchrom UP5 WOD/25M Uptispere 300 5 ODB, 250 mm × 46 mm).

Construction of HIV-1 RT Mutants. The original plasmid pRT66/51 encoding $HIV\text{-}1_{BH10}$ reverse transcriptase (*21*) was kindly provided by R. S. Goody from the Max Planck Institute, Dortmund, Germany. The coding sequence of both p51 and p66 were cloned separately into the pQE30 expression vector (Qiagen Courtaboeuf, France) by digestion of the original plasmid with restriction enzymes *Bam*HI and *Hin*d III. Mutagenesis of both subunits at positions 24 and 61, replacing Trp^{24}, Phe^{61} or both by a glycine residue was performed using the QuikChange site-directed mutagenesis kit (Stratagene, Amsterdam, The Netherlands). The presence of the appropriate substitutions was confirmed by sequencing prior to bacterial expression.

Expression and Purification of Recombinant Proteins. M15 bacteria (Qiagen Courtaboeuf, France) were separately transformed with all the constructs of p51 and p66 subunits. Cells were grown at 37 °C up to about $0.3OD_{595}$, then cultures were cooled to 20 °C and induced overnight with 0.5 mM isopropyl-1-thio-β-D-galactopyranoside. Bacterial cultures expressing His-tagged p66 subunit were mixed with cultures expressing His-tagged p51 subunit to enable dimerization during sonication. For protein isolation and initial purification, the filtered supernatant was applied onto a Hi-Trap chelating column equilibrated with 50 mM sodium phosphate buffer, pH 7.8, containing 150 mM NaCl supplemented with 50 mM imidazole. The heterodimeric form of RT was eluted with an increasing gradient of imidazole, then desalted into 50 mM Tris, pH 7.0, 50 mM NaCl, and 1 mM EDTA (buffer B) by passage through a High Prep Desalting 26/10 column. Fractions containing both p51 and p66 subunits were then loaded onto an anion-exchange HiTrap Q column (Amersham Biosciences, Orsay, France) equilibrated with buffer B, and RT remained in the flow through. After concentration, heterodimeric RT was finally purified by size-exclusion chromatography on a HiLoad 16/60 Superdex 75 column equilibrated with buffer B. Protein concentrations were determined at 280 nm using a molar extinction coefficient of 260 450 $M^{-1}\cdot cm^{-1}$. Proteins were stored at −80 °C in buffer supplemented with 5% glycerol.

Dissociation Kinetics. Dissociation of RTs was achieved by addition of acetonitrile up to 25% in 50 mM 2-(*N*-morpholino)ethanesulfonic acid (MES), pH 6.5, 50 mM KCl, 10 mM $MgCl_2$ buffer, followed by a 2-hour incubation at 25 °C. Experiments were performed using an enzyme concentration of 3 or 5 μM in the absence or in the presence of a 2-fold excess of primer/template (18/36-mer) as previously described (*10*). The establishment of the dissociation equilibrium was followed in a time-dependent manner by monitoring either the increase of the intrinsic protein fluorescence or the decrease of RT polymerase activity. Intrinsic fluorescence excitation was routinely performed at 290 nm, and emission was measured at the wavelength of the greatest intensity change (340 nm). For dissociation kinetics, a protein concentration of 500 nM was used in 50 mM Tris, pH 7.0 and 50 mM NaCl and dissolved in a final concentration of 17% acetonitrile. The data were fitted using a first-order equation with a single rate constant.

Enzyme Activity Assay. RT and p51 monomer polymerase activities were measured in a standard reaction assay using poly(rA)·$(dT)_{15}$ as template/primer as previously described (*6*). Ten microliters (50 ng) of p51 or RT was then incubated at 37 °C for 30 min with 20 μL of reaction buffer (50 mM Tris, pH 8.0, 80 mM KCl, 6 mM $MgCl_2$, 5 mM DTT, 0.15 μM poly(rA−dT), 15 μM dTTP, 0.3 μCi ^{3}H-dTTP). Reactions were stopped by precipitation of nucleic acids with 5 mL of 20% trichloroacetic acid (TCA) solution for 2 h on ice, then filtered using a multiwell sample collector (Millipore), and washed with 5% TCA solution. Filters were dried at 55 °C for several minutes and radionucleotide incorporation was determined by liquid scintillation spectrometry. RT RNase-H activity was measured as previously described (*13*).

Data Analysis. Dissociation data from polymerase activity measurements of heterodimeric RTs were transformed to yield the relative fraction of monomers. We have previously demonstrated that reversible dissociation of HIV-1 RT heterodimer follows a one-step model (*10*). The total concentration of monomers (M_t) at any concentration of acetonitrile can be defined in terms of the fraction of monomeric protein (M_m) based on the polymerase activity measurements, and the K_d can be expressed in terms of measurable values M_t and M_m.

$$K_d = 2M_t(M_m)^2/(1 - M_m) \quad (1)$$

For determination of the free energy of heterodimeric RT dissociation, we used the two-state denaturation model (*22*) where free dissociation energy is defined as a linear function of the concentration of dissociating agent acetonitrile:

$$\Delta G_d = \Delta G_d^{H_2O} + m[A] = -RT \ln K_d \qquad (2)$$

where m is the slope of the plot of ΔG_d versus [A]. [A] is the concentration of acetonitrile; R and T are the gas constant and the absolute temperature, respectively. ΔG_d was calculated from the K_d at the corresponding concentrations of acetonitrile using eq 2. $\Delta G_d^{H_2O}$ is the extrapolated free energy of dissociation in the absence of any dissociating agent.

Fluorescence Experiments. Fluorescence titrations of 6-FAM-labeled primer−template (P/T) with RTs were performed in 50 mM Tris, pH 8.0, 50 mM KCl, 10 mM $MgCl_2$ and 1 mM DTT using a Jobin Yvon-Spex Fluoromax 2 spectrofluorometer (Longjumeau, France) with a thermostated cuvette holder at 25 °C in an 0.5 cm path length quartz cuvette. Excitation was performed at 486 nm with a 2 nm slot, and emission spectra were recorded from 500 to 550 nm with an 8 nm slot. Primer−template sequences, TCCCTGTTCGGGCGCCAC and TGTGGAAAATCTCATGCAGTGGCGCCCGAACAGGGA, respectively, were separately resuspended in water and diluted to 10 μM in annealing buffer, 25 mM Tris, pH 7.5, 50 mM NaCl. Oligonucleotides were mixed together and heated at 95 °C for 2 min, then cooled to room temperature for several hours. A fixed concentration of P/T (15 nM) was titrated with proteins from 1 nM to 1 μM.

HPLC and Fast Protein Liquid Chromatography (FPLC) Size-Exclusion Chromatography. HPLC Chromatography was performed as already described (*6, 16*) using two HPLC columns in series (Bio-Rad TSK-125 and TSK-250, Marnes-la-Coquette, France). Size-exclusion chromatography was performed on a Waters, Breeze software, HPLC system (St-Quentin en-Yvelines, France) with 5−10 μg of protein, and the columns were eluted with 200 mM potassium phosphate (pH 6.8) at a flow rate of 0.8 mL/min. FPLC chromatography was performed on a HiLoad 16/60 Superdex 75 column (Amersham Biosciences) equilibrated with 200 mM potassium phosphate (pH 6.8) with 100 μg of protein or peptide. The column was calibrated using Pharmacia protein markers including albumin (67 kDa), ovalbumin (43 kDa), chymotrypsinogen (25 kDa), and RNase A (13.7 kDa).

Circular Dichroism. CD spectra were collected on a Jasco 810 dichrograph using 1-mm-thick quartz cells at 25 °C. Spectra were scanned between 185 and 260 nm at 10 nm/min with a bandwidth of 1 nm. Experiments were performed with a protein concentration of 3.0 μM.

Biosensor Experiments. All experiments were performed at 25 °C using a Biacore 3000 (Biacore AB, Piscataway, NJ). RTs and p51 subunits were immobilized onto a carboxymethyl dextran sensor chip using *N*-hydroxysuccinimide (NHS)/1-ethyl-3(3-dimethylaminopropyl)carbodiimide (EDC) coupling as described by the manufacturer. Peptide samples were prepared at different concentrations in the range of 50−1000 nM in 50 mM Tris HCl, pH 8.0, buffer containing 150 mM NaCl, 2 mM EDTA, and 50 mM KCl and were injected (30 μL) over the sensor surface at a flow rate of 10 $\mu L \cdot s^{-1}$. After completion of the injection phase, dissociation was performed for 200 s at the same flow rate. The apparent association and dissociation rate constants were calculated using BIA evaluation, version 3.0, and binding curves were fitted using a simple 1:1 Langmuir two-state reaction model.

Molecular Graphics Representation of the Crystal Structure. Coordinates of crystal structures used were downloaded from the Brookhaven Protein Data Bank (codes 1HMV, 1RTV) (*8, 25*). The modeling package Discover/Insight II (MSI Inc., San Diego, CA) and DeLano Scientific LLC PyMol software, version 0.93 (Delano L W Scientific, San Carlos, CA) were used to analyze the structure of RTs.

RESULTS

Pep-7 Interacts with p51 in the Heterodimeric RT Complex. The interaction of Pep-7 with p51 was monitored by both size-exclusion chromatography and surface plasmon resonance (SPR). We first investigated the binding of fluorescently labeled Pep-7 to RT by size-exclusion chromatography. We previously demonstrated that after overnight incubation Pep-7 induces significant dissociation of homo-(p66/p66) and heterodimeric (p51/p66) RT (*20*). Experiments were performed with a p51 concentration of 1 μM, at which it is entirely monomeric and eluted as a single peak at 17 min (Figure 1B). The monomeric form of p51 (1 μM) was incubated in the presence of fluorescein-labeled Pep-7 (2 μM) for 1 h then analyzed by size-exclusion chromatography. As reported in Figure 1A, fluorescently labeled Pep-7 forms stable complexes with p51. A major peak, which contains both p51 and Pep-7, eluted at 17 min, whereas the free excess of fluorescently labelled Pep-7 eluted at 38 min. Binding of Pep-7 to p51 subunit was then investigated using surface plasmon resonance (SPR). Binding curves were recorded by injecting increasing concentrations of Pep-7 onto a flow cell containing immobilized monomeric p51. As reported in Figure 1C, Pep-7 interacts tightly with monomeric p51 with an estimated dissociation constant of 326 ± 12 nM. We were not able to perform similar experiments with monomeric p66 due to its high tendency to form homodimer at the concentration required for titration.

We therefore postulated that one of the major interactions between Pep-7 and RT, occurs within the p51 subunit. The tryptophan-repeat motif in the connection subdomain of HIV RT has been reported to be essential for dimerization of RT (*12, 23*). A detailed analysis of the close contacts of the tryptophan cluster in the crystallographic structure of RT reveals that the aromatic cluster of the connection subdomain of p51 can be extended to two other aromatic residues, Trp^{24} and Phe^{61}, located in the fingers subdomain of p51 (Figure 2A,B). Trp^{24} is partially exposed to the solvent at the surface of p51, close to Trp^{402} and Glu^{399}. In contrast, Phe^{61} is buried inside p51 close to Trp^{402} , Ile^{411}, and Thr^{403}. Sequence alignments of these regions reveal that both residues are extremely well conserved in the different isolates of HIV-1 and HIV-2 (Figure 2C), suggesting that they may both be essential for either the structural organization of the p51 subunit in the dimeric form of RT or the biological activity of RT. To validate this concept, we selectively mutated the p51 subunit either at single residues, $p51^{W24G}$ and $p51^{F61G}$, or simultaneously at both, $p51^{W24G,F61G}$. As a control, similar mutations were introduced into p66. Using these mutants,

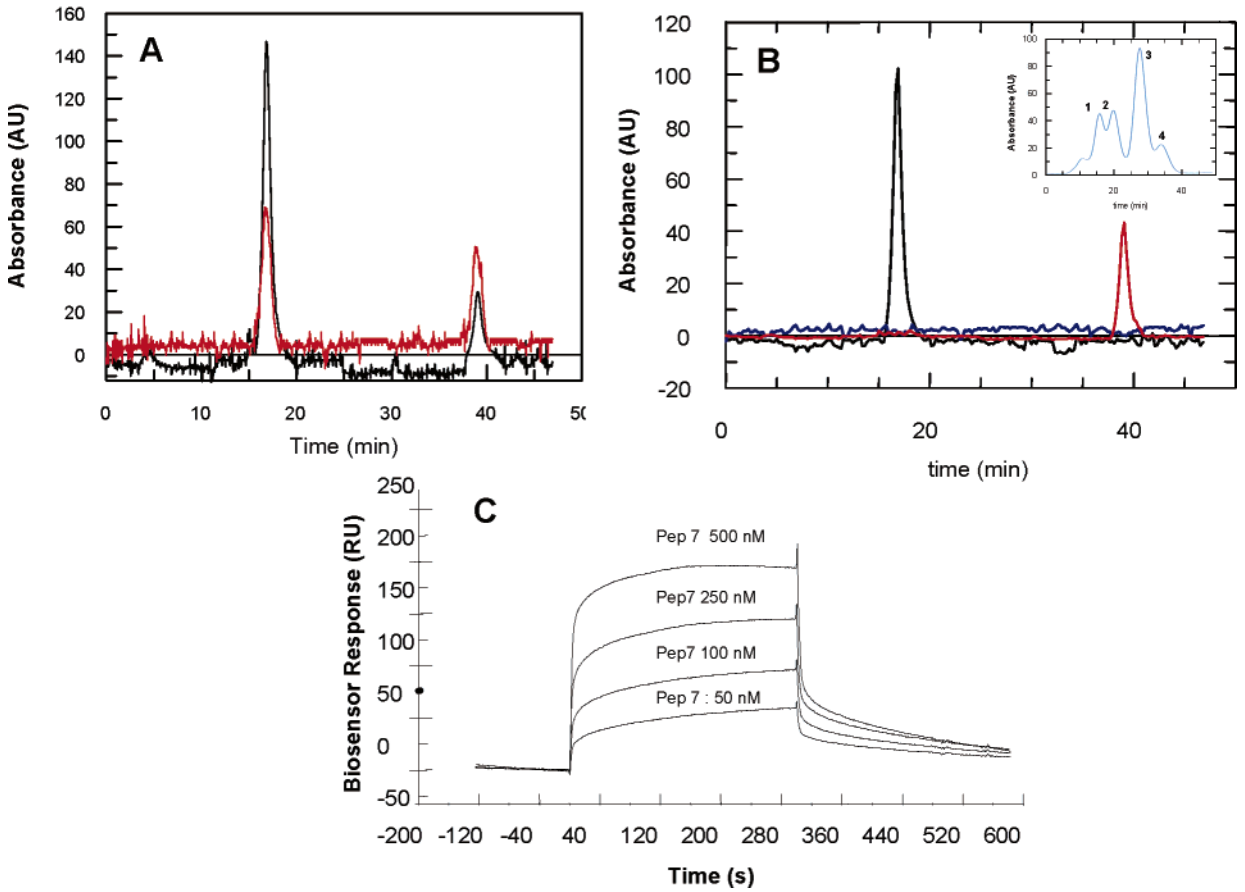

FIGURE 1: Binding of Pep-7 to monomeric p51. In panel A, the formation of Pep-7/p51 complexes were monitored by size-exclusion chromatography. Monomeric p51 (1 μM) was incubated in the presence of Pep-7 (2 μM) for 30 min at 20 °C, then applied onto a size-exclusion HiLoad 16/60 Superdex 75 column and eluted with 200 mM potassium phosphate buffer, pH 6.8. Proteins were monitored at 280 nm (black line) and fluorescein-labeled peptide at 490 nm (red line). In panel B, control experiments were performed with monomeric p51 and Pep-7. In the inset, the column was calibrated using Pharmacia protein markers, including (1) albumin (67 kDa), (2) ovalbumin (43 kDa), (3) chymotrypsinogen (25 kDa), and (4) RNase A (13.7 kDa). Panel C shows binding of Pep-7 to p51 subunit monitored by SPR. Increasing concentrations of Pep-7 were injected over p51 immobilized on the chips. The association and dissociation phase data for a subset of Pep-7 concentrations were fitted using a simple 1:1 Langmuir model using Biacore Evaluation software.

the roles of Trp^{24} and Phe^{61} on the stability and catalytic activity of HIV-1 RT were characterized in detail and the ability of Pep-7 to interact with each of the different mutant forms of RT was investigated.

Mutations of Trp^{24} and Phe^{61} on p51 Do Not Affect the Enzymatic Activities of RT. We first investigated to what extent these mutations of Trp^{24} and Phe^{61} affected the polymerase activity of RT. The effect of each mutation on the affinity of RT for P/T was monitored by equilibrium fluorescence titration using a fluorescently labeled DNA P/T (18/36-mer) labeled at the 5′-end of the primer with the fluorescein derivative 6-FAM as previously described (*24*, *25*). The binding of FAM oligonucleotide to HIV RT led to 51% quenching of the fluorescence of the FAM group (Figure 3A), and a K_d value of 5.4 ± 0.7 nM was determined for the wild-type enzyme, in perfect agreement with previous findings (*24*, *25*). None of the mutations altered binding of the primer/template to RT significantly, as K_d values of 2.6 ± 0.7, 4.4 ± 0.5, and 3.1 ± 0.4 nM were calculated for $p66/p51^{W24G}$, $p66/p51^{F61G}$ and the double mutant $p66/p51^{W24G,F61G}$, respectively. We also demonstrated that these mutations on p51 subunit do not significantly affect polymerase activity (Figure 3B), as well as RNase-H activity (data not shown), of RT in steady-state equilibrium experiments. Only a slight decrease in polymerase activity of 5−10% is observed for the double mutant $p66/p51^{W24G,F61G}$.

p51 Residues Trp^{24} and Phe^{61} Are Involved in Stabilization of the Dimeric Form of RT. We next investigated the impact of both mutations on the structure, the integrity and stability of the dimeric form of HIV-1 RT. We first showed that mutations on the p51 subunit do not alter its overall secondary structure. As reported in Figure 4, $p51^{WT}$ and mutants exhibit similar CD spectra both in shape and ellipticity with two minima at 208 and 222 nm, characteristic of helical proteins. We have previously demonstrated that acetonitrile is a potent agent to monitor RT dissociation in a totally reversible manner (*6*, *12*). We therefore analyzed the dissociation kinetics of the different mutant forms of RT using 17% acetonitrile. Kinetic experiments were performed as described previously (*10*). All dissociation time curves followed monophasic kinetics and were fitted as a single-exponential reaction (Figure 5A). A dissociation rate constant of 7.7×10^{-3} s^{-1} was obtained for wild-type RT, as well as for $p66^{W24G,F616}/p51$, which bears both W24G and F61G mutations on the p66 subunit. In contrast, the dissociation rate increases by 1.4-, 2.1-, and 2.4-fold for $p66/p51^{W24G}$, $p66/p51^{F61G}$, and $p66/p51^{W24G,F61G}$, respectively, indicating that mutations of the p51 subunit increase the dissociation rate of RT and therefore destabilize the dimer in the presence of acetonitrile. To confirm the key role of residues Trp^{24}

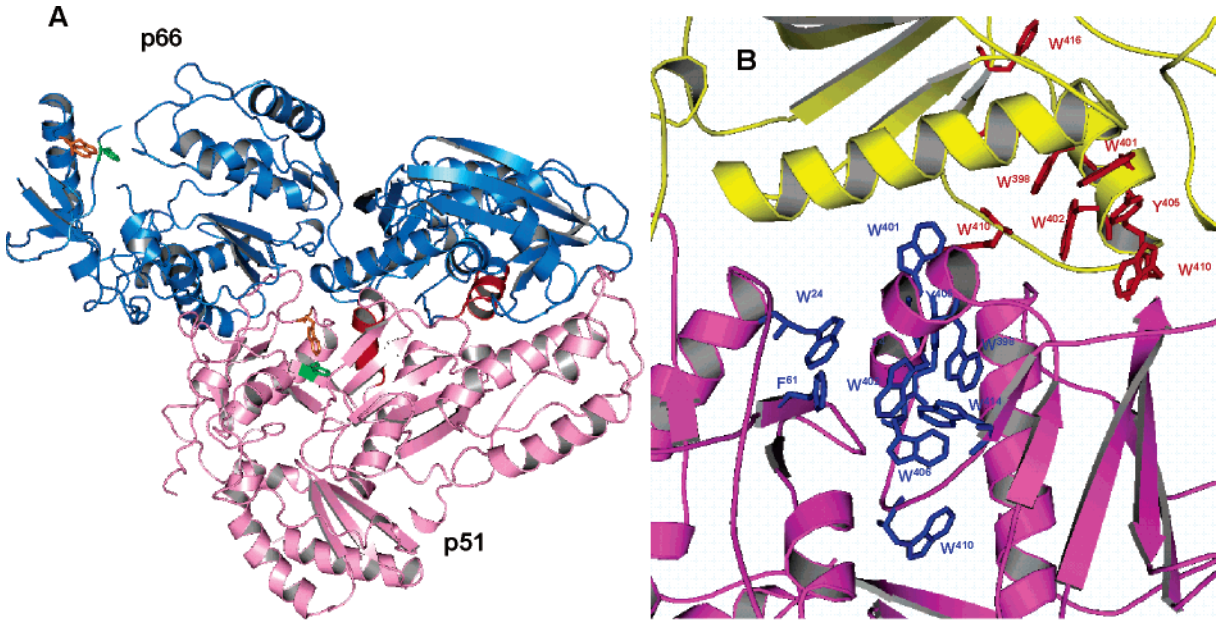

C

	10	20	30	60	70	CLADE
POL_HV1JR	VKLKPGMDGPKVKQWPLTEEKIK	-	-	YNTPVFAIKKKDST		A
POL_HV1MN	VKLKPGMDGPKVKQWPLTEEKIK	-	-	YNTPVFAIKKKDST		B
POL_HV1Y2	VKLKPGMDGPKVKQWPLTEEKIK	-	-	YNTPVFAIKKKDST		C
POL_HV1EL	VKLKPGMDGPKVKQWPLTEEKIK	-	-	YNTPIFAIKKKDST		D
POL_HV1U4	VKLKPEMDGPKVKQWPLTEEKIK	-	-	YNTPVFAIKKKDST		A1
POL_HV1BR	VKLKPGMDGPKVKQWPLTEEKIK	-	-	YNTPVFAIKKKDST		B
POL_HV2RO	IMLKPGKDGPKLRQWPLTKEKIE	-	-	YNTPTFAIKKKDKN		A
POL_HV2G1	VTLKPGKDGPRLRQWPLTKEKIE	-	-	YNTPTFAIKKKDKN		A
Prim.cons.	22LKPGMDGPKV2QWPL2EEKIK	-	-	YNTPVFAIKKKDST		

FIGURE 2: Ribbon diagram of HIV 1 RT and location of the tryptophan-rich domains. Panel A shows a ribbon diagram of the structure of HIV-1 RT. p66 and p51 are in blue and pink, respectively. The position of the tryptophan motif corresponding to Pep-7 is shown in red, Trp^{24} in orange, and Phe^{61} in green. Panel B shows close up of the tryptophan-rich motif of the connection subdomains and location of Trp^{24} and Phe^{61} on p51. Coordinates of crystal structures used were extracted from the Brookhaven Protein Data Bank (code 1HMV, 1RTV). The figures were generated using PyMol software, version 0.93 (Delano L W Scientific, San Carlos, CA). Panel C shows sequence alignments of the fingers subdomain of RT (residues 9−33 and 56−70) in different isolates of HIV-1 and HIV-2.

and Phe^{61} in p51 on the stability of RT, we determined the thermodynamic parameters of the different forms of RT using equilibrium dissociation experiments. Acetonitrile-mediated dissociation of RT was monitored by following the loss of RNA-dependent DNA polymerase activity. These data were correlated with the fraction of monomeric subunits determined by size-exclusion HPLC (Figure 5B). We were able to dissociate all forms of RT reversibly by acetonitrile treatment without inducing unfolding of the monomers or protein precipitation. Dissociation transition curves obtained for all RTs showed a sharp single sigmoidal transition, and complete dissociation was obtained with 22%, 20%, 18%, and 16% acetonitrile with transition midpoint values of 16.8%, 13.5%, 12.4%, and 11% of acetonitrile for p66/p51, $p66/p51^{W24G}$, $p66/p51^{F61G}$, and $p66/p51^{W24G,F61G}$, respectively. The dependency of RT dissociation on enzyme concentration, complete reversibility of this event, and single transition curves obtained are consistent with the fact that acetonitrile induces dissociation of RT according to a two-state model, in which an equilibrium exists between a population of RT dimer (D) and folded monomers (M). Thermodynamic parameters of HIV RT dissociation were calculated according to this model: ΔG_{H_2O} was extrapolated from the free energy to zero acetonitrile concentration, and dissociation constants were calculated from free energy values based on eq 2 (Table 1). $\Delta G_d^{H_2O}$ is reduced to 9.2, 7.5, and 6.8 kcal/mol and dissociation constants to 7.3×10^{-8}, 1.5×10^{-6}, and 5.3×10^{-6} M for $p66/p51^{W24G}$, $p66/p51^{F61G}$, and $p66/p51^{W24G,F61G}$, respectively. These data suggest that major alterations occur when residue Phe^{61} is mutated within p51 and demonstrate that destabilization of RT is slightly increased when both Phe^{61} and Trp^{24} are replaced by a glycine. In contrast no marked change in the stability of RT was observed when these mutations were introduced into the p66 subunit.

To confirm the impact of mutations on the p51 subunit on RT heterodimer stability, similar experiments were performed in the presence of a 2-fold excess of P/T. As previously demonstrated (*10*), P/T binding increased the

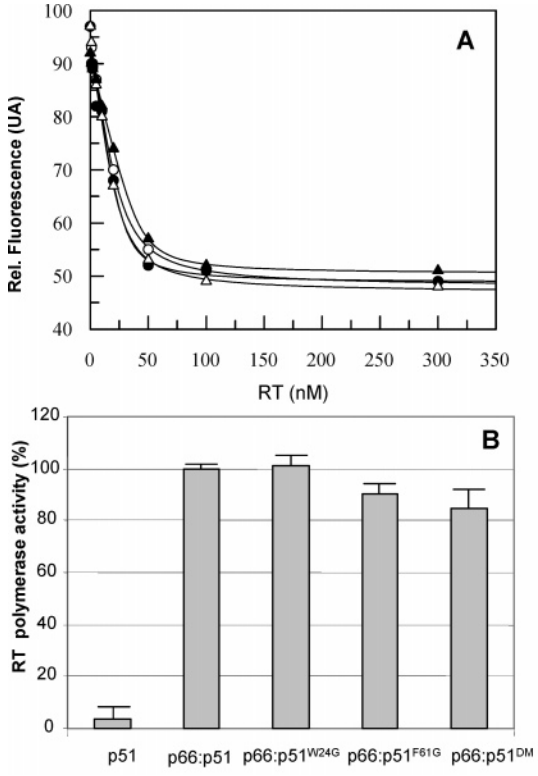

FIGURE 3: Effect of the mutations of Trp^{24} and Phe^{61} on p51 on the polymerase activity of RT. Panel A shows the titration of P/T binding to mutants of RT. The binding of 5′-FAM-labeled primer−template to RT was monitored by following the quenching of extrinsic P/T fluorescence at 521 nm upon excitation at 485 nm. A fixed concentration of 5′-FAM-labeled primer−template (15 nM) was titrated by increasing concentration of p66/p51 (○), p66/$p51^{W24G}$ (●), p66/$p51^{F61G}$ (△), and p66/$p51^{W24G,F61G}$ (▲). Experiments were fitted using quadratic equation as described in ref *26*. Panel B shows the specific polymerase activity of mutants of RT. The polymerase activity of each mutant was evaluated using standard RT activity assays (30 min at 37 °C) and normalized with the value obtained for p66/p51.

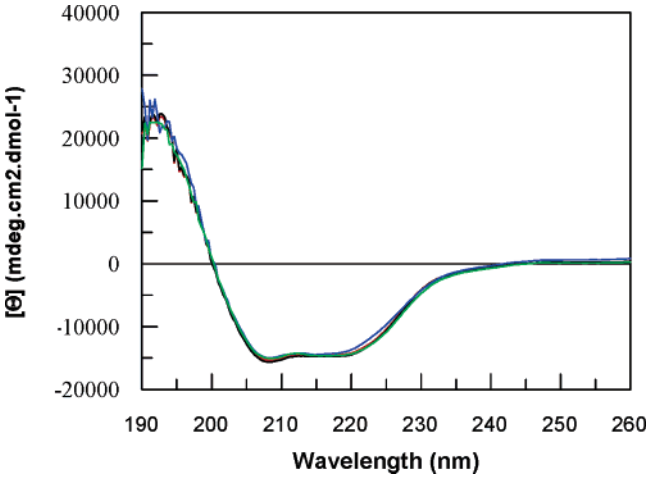

FIGURE 4: CD Spectrum of different mutants of p51. Experiments were performed at 25 °C using a concentration of protein of 3 μM of p51 (red), $p51^{W24G,F61G}$ (blue), $p51^{W24}$ (black), and $p51^{F61G}$ (green).

stability of the p66/p51 heterodimer by 1.2 kcal/mol with a K_d of 8.4×10^{-10} M. Interestingly, P/T binding dramatically increased the stability of p66/$p51^{W24G,F61G}$ by 4.4 kcal/mol with $\Delta G_d^{H_2O}$ of 10.2 ± 0.5 kcal/mol and the binding affinity

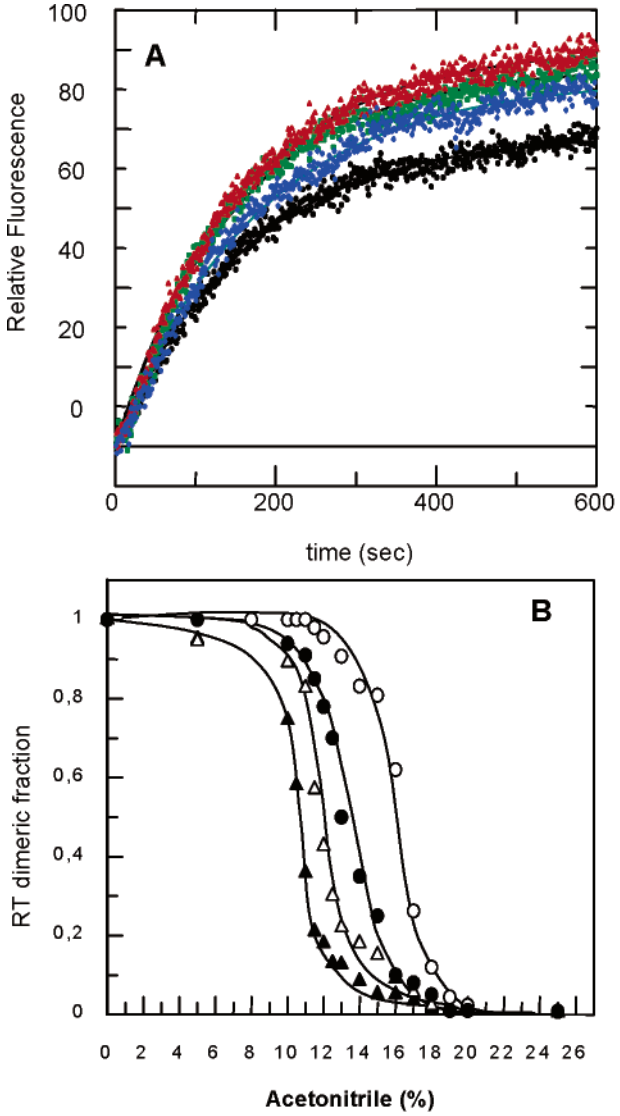

FIGURE 5: Effect of the mutations of Trp^{24} and Phe^{61} on p51 on stability of RT. Panel A shows the kinetics of RT dissociation induced by acetonitrile. p66/p51 (black line), p66/$p51^{W24G}$ (blue line), p66/$p51^{F61G}$ (green line), and p66/$p51^{W24G,F61G}$ (red line) were fully dissociated by adding 17% of acetonitrile at pH 6.8, 25 °C. The kinetics of dissociation were monitored by following the increase of intrinsic fluorescence at 340 nm upon excitation 290 nm. The curves were fitted according to a first-order reaction. Panel B shows the dependence of the monomeric fraction of the different RTs on the acetonitrile concentration. Five micromolar p66/p51 (○), p66/$p51^{W24G}$ (●), p66/$p51^{F61G}$ (△), and p66/$p51^{W24G,F61G}$ (▲) were incubated with different concentrations of acetonitrile (0−25%). Acetonitrile-induced dissociation of RT was monitored by measuring the polymerase activity.

by about 300-fold with a K_d value of 1.2×10^{-8} M (Table 1). These results demonstrate that the decrease of heterodimeric RT integrity associated with mutations W24G and F61G on the p51 subunit are partially compensated by the binding of primer/template.

p51 Residues Trp^{24} and Phe^{61} Are Required for the Binding of Pep-7 to RT. Binding of Pep-7 to monomeric mutants of p51 and different forms of RT was monitored by SPR titration (Figure 6 and Table 2). The different RTs and p51 were cross-linked onto chips by the HNS/EDC coupling strategy and titrated with increasing concentrations of Pep-7 or control peptide, Pep-77. Pep-77 is devoid of tryptophan

Table 1: Thermodynamic Parameters of Acetonitrile-Induced Dissociation Transition of Different HIV RTs[a]

RTs	$\Delta G_d^{H_2O}$ (kcal/mol)	$[ACN]_{1/2}$ (%)	K_d (M)
p66/p51	10.5 ± 0.6	17.6	7.2×10^{-9}
p66/p51 + P/T[b]	11.7 ± 0.4	18.5	8.4×10^{-10}
p66/p51^{W24G}	9.2 ± 0.4	13.5	7.3×10^{-8}
p66/p51^{F61G}	7.5 ± 0.7	12.4	1.5×10^{-6}
p66/p51^{W24G,F61G}	6.8 ± 0.3	11	5.3×10^{-6}
p66/p51^{W24G,F61G} + P/T[b]	10.2 ± 0.5	17.2	1.2×10^{-8}
p66^{W24G,F61G}/p51	10.4 ± 0.5	17.5	8.6×10^{-9}

[a] Dissociation transitions were monitored by polymerase activity assay and size exclusion HPLC. A concentration of 5 μM of heterodimer RT was used, $\Delta G_d^{H_2O}$ and $[ACN]_{1/2}$ were determined from a two-states model analysis of the transition according to eq 1 and the K_d values were calculated using eq 2 (see Experimental Procedures). [b] RTs were incubated with a 2-fold excess of primer/template prior to dissociation.

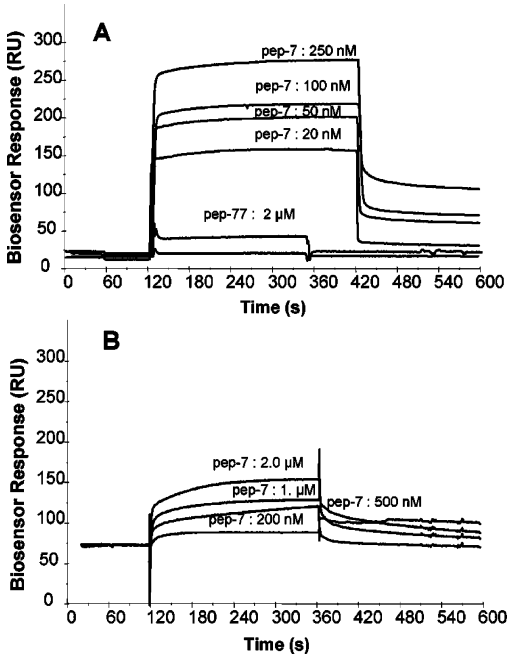

FIGURE 6: Binding of Pep-7 to heterodimeric RT by SPR. Increasing concentrations of Pep-7 or Pep-77 were injected over p66/p51 (panel A) or p66/p51^{W24G,F61G} (panel B) immobilized on the chips. The association and dissociation phase data for a subset of Pep-7 concentrations were fitted using a simple 1:1 Langmuir model using Biacore Evaluation software.

residues and is unable to either interact with RT or block its dimerization. Pep-7 forms stable complexes with heterodimeric (p66/p51) and homodimeric (p66/p66) RTs with dissociation constant estimated to 138 ± 25 and 119 ± 28 nM, respectively, which is similar to values already reported using other approaches (*20*). That Pep-7 strongly interacts with p66/p66 confirms that Pep-7 can inhibit dimerization of both homo- and heterodimeric RTs. The binding of Pep-7 onto both monomeric p51 and RT is dependent on the integrity of p51 residues Trp[24] and Phe[61]. Affinity constant is reduced by 6.7-fold to 2.2 ± 0.2 μM for monomeric p51 harboring the two mutations W24G and F61G and to 470 ± 23 nM, 890 ± 46 nM, and 1.7 ± 0.1 μM for p66/p51^{W24G}, p66/p51^{F61G} and p66/p51^{W24G,F61G}, respectively. In contrast, Pep-7 binding is not affected by mutations on p66 subunits ($K_d = 121 \pm 18$ nM). The difference in the affinity of Pep-7 for p51 monomer and heterodimeric RT may be associated with the fact that in the heterodimer, the interaction of p51 with p66 may stabilize the structure of the p51 subunit and expose the Pep-7 binding site.

Table 2: Binding Constant of Pep-7 for Different p51 Subunits and HIV RTs[a]

RTs	K_d (nM)
p66/p51	138 ± 25
p51	326 ± 12
p66/p66	119 ± 28
p66/p51^{W24G}	470 ± 23
p66/p51^{F61G}	890 ± 46
p66/p51^{W24G,F61G}	1700 ± 120
p51^{W24G,F61G}	2400 ± 200
p66^{W24G,F61G}/p51	121 ± 18

[a] RTs and p51 subunits were immobilized onto a carboxymethyl dextran sensor chip using the HNS/EDC coupling method. The apparent association and dissociation rate constants were calculated using BIA evaluation, version 3.0, and binding curves were fitted using a simple 1:1 Langmuir two-state reaction model.

DISCUSSION

Because the dimeric form of RT is essential for its biological functions, we and other groups have proposed that inhibiting its subunit−subunit assembly constitutes a very attractive approach for the design of a new generation of more specific inhibitors (*14*, *15*). We have designed a peptide inhibitor of 10 residues (Pep-7) derived from the tryptophan cluster of the connection subdomain that abolishes the production of viral particles at nanomolar concentrations (*20*). To improve the design of more powerful inhibitors, it is essential to understand the mechanism through which Pep-7 affects RT dimerization. In the present work, we demonstrate that Pep-7 does not target the subunit−subunit interface directly, that its binding site is located on p51 more specifically within the heterodimer, and that the latter involves two highly conserved residues of the fingers subdomain of p51, Trp[24] and Phe[61].

Several studies have concluded that the p51 subunit plays an essential role in the stabilization of RT. Analysis of the X-ray structure of the subunit interface (*26*−*28*) and of chimeric or truncated RTs (*11*, *29*, *30*) has revealed a significant implication of fingers, palm, and connection subdomains of p51 in the p51/p66 interface. Close examination of RT structures reveals that the two highly conserved residues Trp[24] and Phe[61] in the fingers subdomain of p51 subunit are in close contact with several residues of the connection subdomain. We demonstrate that selective mutagenesis of the Trp[24] and Phe[61] residues of p51 to a glycine dramatically alters the interaction between p51 and p66 and reduces both the stability of the heterodimer and binding of Pep-7 to RT. $\Delta G_d^{H_2O}$ is reduced by 1.3 and 3.0 kcal/mol for RT mutants p51^{W24G} and p51^{F61G}, respectively, and binding of Pep-7 is reduced by 3.4- and 6.2-fold, respectively. Neither Trp[24] nor Phe[61] is located at the subunit interface, but they form close contacts with residues of the connection subdomain, including Trp[402] and Glu[399] for Trp[24] and Trp[402], Thr[403], and Ile[411] for Phe[61]. Interestingly, simultaneous introduction of both mutations results in a more pronounced destabilization of RT (3.7 kcal/mol) and decrease of Pep-7 binding (12-fold). The key role of the tryptophan repeat motif in the connection subdomain of p66 in RT dimerization has been

recently documented. Mutations of Trp^{401} and Trp^{414} have been shown to abolish RT dimerization (*23*). Moreover, the same motif is also involved in the fixation of metalloporphyrins or derivatives, which inhibit RT (*31*). Here we show that the structural integrity of the tryptophan cluster of the connection subdomain of p51 is also a major requirement for RT dimerization. In particular, it becomes clear that the fingers subdomain of p51, especially residues Phe^{61} and Trp^{24}, which are not directly involved in the subunit interface, plays a major role in the heterodimer stability. The implication of the fingers subdomain of p51 in heterodimer formation was also suggested from RT dimerization kinetics (*12*). Moreover, the recent determination of the crystallographic structure of HIV-2 RT reveals structural differences in the fingers subdomain of p55 in comparison to p51 of HIV-1 (*32*), which may explain the greater stability observed for HIV-2 RT dimer (*10*).

We and others have demonstrated that the biological activities of RT are directly associated with the dimeric form of the enzyme. However, although mutations of p51 dramatically affect RT stability, they do not significantly alter RT polymerase and RNase-H activities in steady-state conditions. We have demonstrated that the lack of effect on RT polymerase and RNase-H activities is because primer/template binding partially compensates the decrease of RT stability associated with p51 mutations. The dissociation constant of p66/$p51^{W24G,F61G}$ increases approximately 300-fold in the presence of primer/template. Similar observations were already reported for p66/p51 (*10*), as well as for p51/p51 homodimer, which can be observed only in the presence of primer/template due to the low binding constant in the millimolar range (*33*, *34*). In contrast, mutation of Phe^{61} in p66 dramatically affects strand displacement activity as well as RT processivity (*35*). These results point to the important role of Phe^{61} on both subunits and its implication in conformational and catalytic properties of RT.

Both size-exclusion chromatography and SPR experiments lead to the conclusion that Pep-7 interacts tightly with monomeric p51 subunit (K_d = 380 nM), as well as with the dimeric form of RT (K_d = 120−140 nM). The similarity between those values and the ones obtained using other techniques validate the use of SPR to monitor binding of Pep-7 to RT (*20*). $p51^{W24G}$ and $p51^{F61G}$ mutants in both monomeric p51 and heterodimeric RT exhibited a significantly reduced binding to the peptide inhibitor. As observed for stability of RT, this effect is highly selective of p51 because none of these mutations in p66 affect binding of Pep-7. The impact on Pep-7 binding was more marked with $p51^{F61G}$ than with $p51^{W24G}$, and an even greater decrease in binding was obtained with $p51^{W24G,F61G}$, suggesting that both residues are involved in the binding site of the inhibitor and that there is a direct correlation between destabilization of the RT dimer and Pep-7 binding. Taken together, our results suggest that Pep-7 interacts first with p51 within the heterodimer, in a cleft located between the fingers and connection subdomains of p51, which is exposed upon binding to p66 and remains accessible in the presence of P/T (Figure 7). Binding of Pep-7 to p51 promotes a conformational change, which destabilizes RT dimer conformation, thereby triggering dissociation. Destabilization of the dimer is associated with disruption of the close contacts between the fingers and the connection subdomains of p51 involving Trp^{24} and Phe^{61}. However, we cannot exclude that mutation of Trp^{24} and Phe^{61} indirectly disrupts the Pep-7 binding site.

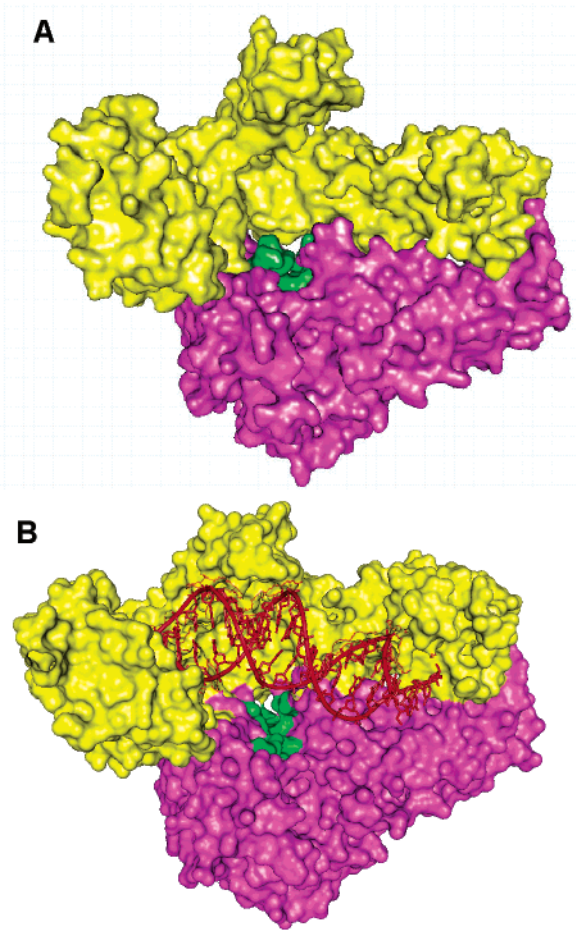

FIGURE 7: Location of the postulated Pep-7 binding site in the structure of HIV RT. p66 and p51 subunits are in yellow and magenta, respectively. The cleft located between the fingers and connection subdomains of p51 is shown in green on the structures of RT (A) and of RT−primer/template complex (B).

Based on its proposed mechanism of action, Pep-7 inhibitor can be assimilated to a class of small molecules that bind close to the dimer interface of RT and impact on the overall stability of the heterodimeric complex (*14*−*17*). Similarly, NNRTIs such as TSAO-T or compounds derived from *N*-(4-*tert*-butylbenzoyl)-2-hydroxy-1-naphthaldehyde hydrazone (BBNH) partially interact with p51 and have been shown to decrease the stability of RT (*17*, *18*). Interestingly, resistance to TSAO-T has been associated with the E138K mutation in p51, which constitutes one of the unique mutation conferring resistance to NNRTI reported on p51 (*36*). In contrast, other NNRTIs (EFV, Nevirapin, UC781) that do not directly interact with p51 tend to promote dimer formation (*19*). A recent study suggests that binding of these NNRTIs induces conformational reorganization of the p66 subunit, which mainly implicates the fingers subdomain (*37*). These studies lead to the conclusion that binding of NNRTIs impact dimeric RT by interacting with or affecting residues in the fingers subdomains of p51 or p66.

In conclusion, we have shown that Pep-7 constitutes a potent inhibitor of RT, which binds p51 subunit within the heterodimer and induces a conformational change followed

by RT dissociation. That Pep-7 interacts similarly with both p51/p66 and p66/p66 may explain the high efficiency of this peptide in suppressing HIV replication (*20*) and supports the hypothesis that one of the p66 subunits adopts a p51 like conformation in the p66/p66 homodimer. It was recently reported that formation of heterodimeric RT requires first formation of a p66/p66 homodimer, which is then processed by protease (*38*). Indeed in infected cells, Pep-7 can potentially interact with p66/p51 at the early stage of infection and with p66/p66 during formation of RT at a later stage of the infective cycle. Considering the low stability of the p66/p66 homodimer (*25*) and the fact that Pep-7 is able to induce its dissociation (*16*), we postulate that homodimeric RT (p66/p66) constitutes the major target of Pep-7 in vivo.

ACKNOWLEDGMENT

We are grateful to M. C. Morris and F. Heitz for critical reading of the manuscript and helpful discussions. We also thank R. S. Goody for fruitful discussions and RT clones and C. Lionne and S. Marechal for their assistance in spectroscopy.

REFERENCES

1. De Clercq E. (2002) Strategies in the design of antiviral drugs, *Nat. Rev. Drug Discov. 1*, 13−25.
2. Richman, D. D. (1996) Antiretroviral drug resistance: mechanisms, pathogenesis, clinical significance, *Adv. Exp. Med. Biol. 394*, 383−395.
3. Parniak, M. A., and Sluis-Cremer, N. (2000) Inhibitors of HIV-1 Reverse Transcriptase, *Adv. Pharmacol. 49*, 67−109.
4. Menendez-Arias, L. (2002) Targeting HIV: antiretroviral therapy and development of drug resistance, *Trends Pharmacol. Sci. 23*, 381−388.
5. di Marzo Veronese, F., Copeland, T. D., DeVico, A. L., Rahman, R., Oroszlan, S., Gallo, R. C., and Sarngadharan, M. G. (1986) Characterization of highly immunogenic p66/p51 as the reverse transcriptase of HTLV−III/LAV, *Science 231*, 1289−1291.
6. Restle, T., Müller, B., and Goody, R. S. (1990) Dimerization of human immunodeficiency virus type 1 reverse transcriptase. A target for chemotherapeutic intervention, *J. Biol. Chem. 265*, 8986−8988.
7. Kohlstaedt, L. A., Wang, J., Friedman, J. M., Rice, P. A., and Steitz, T. A. (1992) Crystal structure at 3.5 A resolution of HIV-1 reverse transcriptase complexed with an inhibitor, *Science 256*, 1783−1790.
8. Jacobo-Molina, A., Ding, J., Nanni, R. G., Clark, A. D. Jr., Lu, X., Tantillo, C., Williams, R. L., Kamer, G., Ferris, A. L., Clark, P., Hizi, A., Hughes, S. H., and Arnold, E. (1993) Crystal structure of human immunodeficiency virus type 1 reverse transcriptase complexed with double stranded DNA at 3.0 Å resolution shows bent DNA, *Proc. Natl. Acad. Sci. U.S.A. 90*, 6320−6324.
9. Debyser, Z., and De Clercq, E. (1996) Chemical cross-linking of the subunits of HIV-1 reverse transcriptase, *Protein Sci. 5*, 278−286.
10. Divita, G., Rittinger K., Restle T., Immendorfer U., and Goody R. S. (1995) Conformational stability of dimeric HIV-1 and HIV-2 reverse transcriptases, *Biochemistry 34*, 16337−16346.
11. Tachedjian G., Aronson H. E., and Goff S. P. (2000) Analysis of mutations and suppressors affecting interactions between the subunits of the HIV type 1 reverse transcriptase, *Proc. Natl. Acad. Sci. U.S.A. 97*, 6334−6339.
12. Divita, G., Rittinger, K., Geourjon, C., Deleage, G., and Goody, R. S. (1995) Dimerization kinetics of HIV-1 and HIV-2 reverse transcriptase: a two step process, *J. Mol. Biol. 245*, 508−521.
13. Restle, T., Müller, B., and Goody, R. S. (1992) RNase H activity of HIV reverse transcriptases is confined exclusively to the dimeric forms, *FEBS Lett. 300* (1), 97−100.
14. Divita, G., Restle, T., Goody, R. S., Chermann, J. C., and Baillon, J. G. (1994) Inhibition of human immunodeficiency virus type 1 reverse transcriptase dimerization using synthetic peptides derived from the connection domain, *J. Biol. Chem. 269*, 13080−13083.
15. Sluis-Cremer, N., and Tachedjian, G. (2002) Modulation of the oligomeric structures of HIV-1 retroviral enzymes by synthetic peptides and small molecules, *Eur. J. Biochem. 269*, 5103−5111.
16. Divita, G., Baillon, J. G., Rittinger, K., Chermann, J. C., and Goody, R. S. (1995) Interface peptides as structure-based human immunodeficiency virus reverse transcriptase inhibitors, *J. Biol. Chem. 270*, 28642−28646.
17. Sluis-Cremer, N., Arion, D., and Parniak, M. A. (2002) Destabilization of HIV-1 reverse transcriptase dimer upon interaction with N-acyl hydrazone inhibitors, *Mol. Pharmacol. 62*, 398−405.
18. Sluis-Cremer, N., Dmitrienko, G. I., Balzarini, J., Camarasa, M. J., and Parniak, M. A. (2000) Human immunodeficiency virus type 1 reverse transcriptase dimer destabilization by 1-[Spiro[4″-amino-2″,2″-dioxo-1″,2″-oxathiole-5″,3′-[2′,5′-bis-*O*-(*tert*-butyldimethylsilyl)-*β*-D-ribofuranosyl]]]-3-ethylthymine, *Biochemistry 39*, 1427−1433.
19. Tachedjian, G., Orlova, M., Sarafianos, S. G., Arnold, E., and Goff, S. P. (2001) Nonnucleoside reverse transcriptase inhibitors are chemical enhancers of dimerization of the HIV type 1 reverse transcriptase, *Proc. Natl. Acad. Sci. U.S.A. 98*, 7188−7193.
20. Morris, M. C., Robert-Hebmann, V., Chaloin, L., Mery, J., Heitz, F., Devaux, C., Goody, R. S., and Divita, G. (1999) A new potent HIV-1 reverse transcriptase inhibitor: a synthetic peptide derived from the interface subunit domain, *J. Biol. Chem. 274*, 24941−24946.
21. Müller, B., Restle, T., Weiss, S., Gautel, M., Sczakiel, G., and Goody, R. S. (1989) Coexpression of the subunits of the heterodimer of HIV-1 reverse transcriptase in *Escherichia coli*, *J. Biol. Chem. 264*, 13975−13978.
22. Pace, C. N. (1985) Evaluating contribution of hydrogen bonding and hydrophobic bonding to protein folding, *Methods Enzymol. 131*, 266−280.
23. Tachedjian, G., Aronson, H. E., de los Santos, M., Seehra, J., McCoy, J. M., and Goff, S. P. (2003) Role of the residues in the tryptophan repeat motif for HIV-1 reverse transcriptase dimerization, *J. Mol. Biol. 326*, 381−396.
24. Wöhrl, B. M., Krebs, R., Thrall, S. H., Le Grice, S. F. J., Scheidig, A. J., and Goody, R. S. (1997) Kinetic analysis of four HIV-1 reverse transcriptase enzymes mutated in the primer grip region of p66. Implications for DNA synthesis and dimerization, *J. Biol. Chem. 272*, 17581−17587.
25. Divita, G., Müller, B., Immendorfer, U., Gautel, M., Rittinger, K., Restle, T., and Goody, R. S. (1993) Kinetics of interaction of HIV reverse transcriptase with primer/template, *Biochemistry 32*, 7966−7971.
26. Wang, J., Smerdon, S. J., Jager, J., Kohlstaedt, L. A., Rice, P. A., Friedman, J. M., and Steitz, T. A. (1994) Structural basis of asymmetry in the human immunodeficiency virus type 1 reverse transcriptase heterodimer, *Proc. Natl. Acad. Sci. U.S.A. 91*, 7242−7246.
27. Rodgers, D. W., Gamblin, S. J., Harris B. A., Ray S., Culp J. S., Hellmig B., Woolf D. J., Debouck C., and Harrison S. C. (1995) The structure of unliganded reverse transcriptase from the human immunodeficiency virus type 1, *Proc. Natl. Acad. Sci. U.S.A. 92*, 1222−1226.
28. Hsiou, Y., Ding, J., Das, K., Clark, A. D., Jr., Hughes, S. H., and Arnold, E. (1996) Structure of unliganded HIV-1 reverse transcriptase at 2.7 Å resolution: implications of conformational changes for polymerization and inhibition mechanisms, *Structure 4*, 853−860.
29. Menendez-Arias, L., Abraha, A., Quinones-Mateu, M. E., Mas, A., Camarasa, M. J., and Arts, E. J. (2001) Functional characterization of chimeric reverse transcriptases with polypeptide subunits of highly divergent HIV-1 group M and O strains, *J. Biol. Chem. 276*, 27470−92747.
30. Jacques, P. S., Wöhrl, B. M., Howard, K. J., and Le Grice, S. F. (1994) Mutating the "primer grip" of p66 HIV-1 reverse transcriptase implicates tryptophan-229 in template-primer utilization, *J. Biol. Chem. 269*, 1388−1393.
31. Argyris, E. G., Vanderkooi, J. M., Venkateswaran, P. S., Kay, B. K., and Paterson, Y. (1999) The connection domain is implicated in metalloporphyrin binidng and inhibition of HIV reverse transcriptase, *J. Biol. Chem. 274*, 1549−1556.
32. Ren, J., Bird, L. E., Chamberlain, P. P., Stewart-Jones, G. B., Stuart, D. I., and Stammers, D. K. (2002) Structure of HIV-2 reverse transcriptase at 2.35 Å resolution and the mechanism of resistance to nonnucleoside inhibitors, *Proc. Natl. Acad. Sci. U.S.A. 99*, 14410−14415.

33. Bavand, M. R., Wagner, R., and Richmond, T. J. (1993) HIV-1 reverse transcriptase: Polymerization properties of the p51 homodimer compared to the p66/p51 heterodimer, *Biochemistry 32*, 10543−10552.
34. Sluis-cremer, N., Kempner, E., and Parniak, M. (2003) Structure−activity relationships in HIV-1 reverse transcriptase revealed by radiation target analysis, *Protein Sci. 12*, 2081−2086.
35. Fisher, T. S., Darden, T., and Prasad, V. R. (2003) Substitutions at Phe61 in the beta3-beta4 hairpin of HIV-1 reverse transcriptase reveal a role for the Fingers subdomain in strand displacement DNA synthesis, *J. Mol. Biol. 325*, 443−459.
36. Rodriguez-Barrios, F., Perez, C., Lobaton, E., Velazquez, S., Chamorro, C., San-Felix, A., Perez-Perez, M. J., Camarasa, M. J., Pelemans, H., Balzarini, J., and Gago, F. (2001) Identification of a putative binding site for [2′,5′-bis-*O*-(*tert*-butyldimethylsilyl)-*β*-D-ribofuranosyl]-3′-spiro-5″-(4″-amino-1″,2″-oxathiole-2″,2″-dioxide)thymine (TSAO) derivatives at the p51−p66 interface of HIV-1 reverse transcriptase, *J. Med. Chem. 44*, 1853−1865.
37. Peletskaya, E. N., Kogon, A. A., Tuske, S., Arnold, E., and Hughes, S. H. (2004) Nonnucleoside inhibitors binding affects the interactions of the finger subdomain of human immunodeficiency virus type 1 reverse transcriptase with DNA, *J. Virol. 78*, 3387−3397.
38. Sluis-Cremer, N., Arion, D., Abram, M. E., and Parniak, M. A. (2004) Proteolytic processing of an HIV-1 pol polyprotein precursor: insights into the mechanism of reverse transcriptase p66/p51 heterodimer formation, *Int. J. Biochem. Cell Biol. 36*, 1836−1847.

BI0484264